Measurement of the $B^0 \to \phi K^{*0}$ Decay Amplitudes

B. Aubert,[1] R. Barate,[1] D. Boutigny,[1] F. Couderc,[1] J.-M. Gaillard,[1] A. Hicheur,[1] Y. Karyotakis,[1] J. P. Lees,[1] V. Tisserand,[1]
A. Zghiche,[1] A. Palano,[2] A. Pompili,[2] J. C. Chen,[3] N. D. Qi,[3] G. Rong,[3] P. Wang,[3] Y. S. Zhu,[3] G. Eigen,[4] I. Ofte,[4]
B. Stugu,[4] G. S. Abrams,[5] A. W. Borgland,[5] A. B. Breon,[5] D. N. Brown,[5] J. Button-Shafer,[5] R. N. Cahn,[5] E. Charles,[5]
C. T. Day,[5] M. S. Gill,[5] A. V. Gritsan,[5] Y. Groysman,[5] R. G. Jacobsen,[5] R. W. Kadel,[5] J. Kadyk,[5] L. T. Kerth,[5]
Yu. G. Kolomensky,[5] G. Kukartsev,[5] G. Lynch,[5] L. M. Mir,[5] P. J. Oddone,[5] T. J. Orimoto,[5] M. Pripstein,[5] N. A. Roe,[5]
M. T. Ronan,[5] V. G. Shelkov,[5] W. A. Wenzel,[5] M. Barrett,[6] K. E. Ford,[6] T. J. Harrison,[6] A. J. Hart,[6] C. M. Hawkes,[6]
S. E. Morgan,[6] A. T. Watson,[6] M. Fritsch,[7] K. Goetzen,[7] T. Held,[7] H. Koch,[7] B. Lewandowski,[7] M. Pelizaeus,[7]
M. Steinke,[7] J. T. Boyd,[8] N. Chevalier,[8] W. N. Cottingham,[8] M. P. Kelly,[8] T. E. Latham,[8] F. F. Wilson,[8]
T. Cuhadar-Donszelmann,[9] C. Hearty,[9] N. S. Knecht,[9] T. S. Mattison,[9] J. A. McKenna,[9] D. Thiessen,[9] A. Khan,[10]
P. Kyberd,[10] L. Teodorescu,[10] A. E. Blinov,[11] V. E. Blinov,[11] V. P. Druzhinin,[11] V. B. Golubev,[11] V. N. Ivanchenko,[11]
E. A. Kravchenko,[11] A. P. Onuchin,[11] S. I. Serednyakov,[11] Yu. I. Skovpen,[11] E. P. Solodov,[11] A. N. Yushkov,[11] D. Best,[12]
M. Bruinsma,[12] M. Chao,[12] I. Eschrich,[12] D. Kirkby,[12] A. J. Lankford,[12] M. Mandelkern,[12] R. K. Mommsen,[12]
W. Roethel,[12] D. P. Stoker,[12] C. Buchanan,[13] B. L. Hartfiel,[13] S. D. Foulkes,[14] J. W. Gary,[14] B. C. Shen,[14] K. Wang,[14]
D. del Re,[15] H. K. Hadavand,[15] E. J. Hill,[15] D. B. MacFarlane,[15] H. P. Paar,[15] Sh. Rahatlou,[15] V. Sharma,[15]
J. W. Berryhill,[16] C. Campagnari,[16] B. Dahmes,[16] O. Long,[16] A. Lu,[16] M. A. Mazur,[16] J. D. Richman,[16] W. Verkerke,[16]
T. W. Beck,[17] A. M. Eisner,[17] C. A. Heusch,[17] J. Kroseberg,[17] W. S. Lockman,[17] G. Nesom,[17] T. Schalk,[17] B. A. Schumm,[17]
A. Seiden,[17] P. Spradlin,[17] D. C. Williams,[17] M. G. Wilson,[17] J. Albert,[18] E. Chen,[18] G. P. Dubois-Felsmann,[18]
A. Dvoretskii,[18] D. G. Hitlin,[18] I. Narsky,[18] T. Piatenko,[18] F. C. Porter,[18] A. Ryd,[18] A. Samuel,[18] S. Yang,[18] S. Jayatilleke,[19]
G. Mancinelli,[19] B. T. Meadows,[19] M. D. Sokoloff,[19] T. Abe,[20] F. Blanc,[20] P. Bloom,[20] S. Chen,[20] W. T. Ford,[20]
U. Nauenberg,[20] A. Olivas,[20] P. Rankin,[20] J. G. Smith,[20] J. Zhang,[20] L. Zhang,[20] A. Chen,[21] J. L. Harton,[21] A. Soffer,[21]
W. H. Toki,[21] R. J. Wilson,[21] Q. L. Zeng,[21] D. Altenburg,[22] T. Brandt,[22] J. Brose,[22] M. Dickopp,[22] E. Feltresi,[22]
A. Hauke,[22] H. M. Lacker,[22] R. Müller-Pfefferkorn,[22] R. Nogowski,[22] S. Otto,[22] A. Petzold,[22] J. Schubert,[22]
K. R. Schubert,[22] R. Schwierz,[22] B. Spaan,[22] J. E. Sundermann,[22] D. Bernard,[23] G. R. Bonneaud,[23] F. Brochard,[23]
P. Grenier,[23] S. Schrenk,[23] Ch. Thiebaux,[23] G. Vasileiadis,[23] M. Verderi,[23] D. J. Bard,[24] P. J. Clark,[24] D. Lavin,[24]
F. Muheim,[24] S. Playfer,[24] Y. Xie,[24] M. Andreotti,[25] V. Azzolini,[25] D. Bettoni,[25] C. Bozzi,[25] R. Calabrese,[25]
G. Cibinetto,[25] E. Luppi,[25] M. Negrini,[25] L. Piemontese,[25] A. Sarti,[25] E. Treadwell,[26] F. Anulli,[27] R. Baldini-Ferroli,[27]
A. Calcaterra,[27] R. de Sangro,[27] G. Finocchiaro,[27] P. Patteri,[27] I. M. Peruzzi,[27] M. Piccolo,[27] A. Zallo,[27] A. Buzzo,[28]
R. Capra,[28] R. Contri,[28] G. Crosetti,[28] M. Lo Vetere,[28] M. Macri,[28] M. R. Monge,[28] S. Passaggio,[28] C. Patrignani,[28]
E. Robutti,[28] A. Santroni,[28] S. Tosi,[28] S. Bailey,[29] G. Brandenburg,[29] K. S. Chaisanguanthum,[29] M. Morii,[29] E. Won,[29]
R. S. Dubitzky,[30] U. Langenegger,[30] W. Bhimji,[31] D. A. Bowerman,[31] P. D. Dauncey,[31] U. Egede,[31] J. R. Gaillard,[31]
G. W. Morton,[31] J. A. Nash,[31] M. B. Nikolich,[31] G. P. Taylor,[31] M. J. Charles,[32] G. J. Grenier,[32] U. Mallik,[32] J. Cochran,[33]
H. B. Crawley,[33] J. Lamsa,[33] W. T. Meyer,[33] S. Prell,[33] E. I. Rosenberg,[33] A. E. Rubin,[33] J. Yi,[33] M. Biasini,[34]
R. Covarelli,[34] M. Pioppi,[34] M. Davier,[35] X. Giroux,[35] G. Grosdidier,[35] A. Höcker,[35] S. Laplace,[35] F. Le Diberder,[35]
V. Lepeltier,[35] A. M. Lutz,[35] T. C. Petersen,[35] S. Plaszczynski,[35] M. H. Schune,[35] L. Tantot,[35] G. Wormser,[35]
C. H. Cheng,[36] D. J. Lange,[36] M. C. Simani,[36] D. M. Wright,[36] A. J. Bevan,[37] C. A. Chavez,[37] J. P. Coleman,[37]
I. J. Forster,[37] J. R. Fry,[37] E. Gabathuler,[37] R. Gamet,[37] D. E. Hutchcroft,[37] R. J. Parry,[37] D. J. Payne,[37] R. J. Sloane,[37]
C. Touramanis,[37] J. J. Back,[38,*] C. M. Cormack,[38] P. F. Harrison,[38,*] F. Di Lodovico,[38] G. B. Mohanty,[38,*] C. L. Brown,[39]
G. Cowan,[39] R. L. Flack,[39] H. U. Flaecher,[39] M. G. Green,[39] P. S. Jackson,[39] T. R. McMahon,[39] S. Ricciardi,[39]
F. Salvatore,[39] M. A. Winter,[39] D. Brown,[40] C. L. Davis,[40] J. Allison,[41] N. R. Barlow,[41] R. J. Barlow,[41] P. A. Hart,[41]
M. C. Hodgkinson,[41] G. D. Lafferty,[41] A. J. Lyon,[41] J. C. Williams,[41] A. Farbin,[42] W. D. Hulsbergen,[42] A. Jawahery,[42]
D. Kovalskyi,[42] C. K. Lae,[42] V. Lillard,[42] D. A. Roberts,[42] G. Blaylock,[43] C. Dallapiccola,[43] K. T. Flood,[43]
S. S. Hertzbach,[43] R. Kofler,[43] V. B. Koptchev,[43] T. B. Moore,[43] S. Saremi,[43] H. Staengle,[43] S. Willocq,[43] R. Cowan,[44]
G. Sciolla,[44] S. J. Sekula,[44] F. Taylor,[44] R. K. Yamamoto,[44] D. J. J. Mangeol,[45] P. M. Patel,[45] S. H. Robertson,[45]
A. Lazzaro,[46] V. Lombardo,[46] F. Palombo,[46] J. M. Bauer,[47] L. Cremaldi,[47] V. Eschenburg,[47] R. Godang,[47] R. Kroeger,[47]
J. Reidy,[47] D. A. Sanders,[47] D. J. Summers,[47] H. W. Zhao,[47] S. Brunet,[48] D. Côté,[48] P. Taras,[48] H. Nicholson,[49]
N. Cavallo,[50,†] F. Fabozzi,[50,†] C. Gatto,[50] L. Lista,[50] D. Monorchio,[50] P. Paolucci,[50] D. Piccolo,[50] C. Sciacca,[50]
M. Baak,[51] H. Bulten,[51] G. Raven,[51] H. L. Snoek,[51] L. Wilden,[51] C. P. Jessop,[52] J. M. LoSecco,[52] T. Allmendinger,[53]
K. K. Gan,[53] K. Honscheid,[53] D. Hufnagel,[53] H. Kagan,[53] R. Kass,[53] T. Pulliam,[53] A. M. Rahimi,[53] R. Ter-Antonyan,[53]

Q. K. Wong,[53] J. Brau,[54] R. Frey,[54] O. Igonkina,[54] C. T. Potter,[54] N. B. Sinev,[54] D. Strom,[54] E. Torrence,[54] F. Colecchia,[55]
A. Dorigo,[55] F. Galeazzi,[55] M. Margoni,[55] M. Morandin,[55] M. Posocco,[55] M. Rotondo,[55] F. Simonetto,[55] R. Stroili,[55]
G. Tiozzo,[55] C. Voci,[55] M. Benayoun,[56] H. Briand,[56] J. Chauveau,[56] P. David,[56] Ch. de la Vaissière,[56] L. Del Buono,[56]
O. Hamon,[56] M. J. J. John,[56] Ph. Leruste,[56] J. Malcles,[56] J. Ocariz,[56] M. Pivk,[56] L. Roos,[56] S. T'Jampens,[56] G. Therin,[56]
P. F. Manfredi,[57] V. Re,[57] P. K. Behera,[58] L. Gladney,[58] Q. H. Guo,[58] J. Panetta,[58] C. Angelini,[59] G. Batignani,[59]
S. Bettarini,[59] M. Bondioli,[59] F. Bucci,[59] G. Calderini,[59] M. Carpinelli,[59] F. Forti,[59] M. A. Giorgi,[59] A. Lusiani,[59]
G. Marchiori,[59] F. Martinez-Vidal,[59,‡] M. Morganti,[59] N. Neri,[59] E. Paoloni,[59] M. Rama,[59] G. Rizzo,[59] F. Sandrelli,[59]
J. Walsh,[59] M. Haire,[60] D. Judd,[60] K. Paick,[60] D. E. Wagoner,[60] N. Danielson,[61] P. Elmer,[61] Y. P. Lau,[61] C. Lu,[61]
V. Miftakov,[61] J. Olsen,[61] A. J. S. Smith,[61] A. V. Telnov,[61] F. Bellini,[62] G. Cavoto,[61,62] R. Faccini,[62] F. Ferrarotto,[62]
F. Ferroni,[62] M. Gaspero,[62] L. Li Gioi,[62] M. A. Mazzoni,[62] S. Morganti,[62] M. Pierini,[62] G. Piredda,[62] F. Safai Tehrani,[62]
C. Voena,[62] S. Christ,[63] G. Wagner,[63] R. Waldi,[63] T. Adye,[64] N. De Groot,[64] B. Franek,[64] N. I. Geddes,[64] G. P. Gopal,[64]
E. O. Olaiya,[64] R. Aleksan,[65] S. Emery,[65] A. Gaidot,[65] S. F. Ganzhur,[65] P.-F. Giraud,[65] G. Hamel de Monchenault,[65]
W. Kozanecki,[65] M. Legendre,[65] G. W. London,[65] B. Mayer,[65] G. Schott,[65] G. Vasseur,[65] Ch. Yèche,[65] M. Zito,[65]
M. V. Purohit,[66] A. W. Weidemann,[66] J. R. Wilson,[66] F. X. Yumiceva,[66] D. Aston,[67] R. Bartoldus,[67] N. Berger,[67]
A. M. Boyarski,[67] O. L. Buchmueller,[67] R. Claus,[67] M. R. Convery,[67] M. Cristinziani,[67] G. De Nardo,[67] D. Dong,[67]
J. Dorfan,[67] D. Dujmic,[67] W. Dunwoodie,[67] E. E. Elsen,[67] S. Fan,[67] R. C. Field,[67] T. Glanzman,[67] S. J. Gowdy,[67]
T. Hadig,[67] V. Halyo,[67] C. Hast,[67] T. Hryn'ova,[67] W. R. Innes,[67] M. H. Kelsey,[67] P. Kim,[67] M. L. Kocian,[67]
D. W. G. S. Leith,[67] J. Libby,[67] S. Luitz,[67] V. Luth,[67] H. L. Lynch,[67] H. Marsiske,[67] R. Messner,[67] D. R. Muller,[67]
C. P. O'Grady,[67] V. E. Ozcan,[67] A. Perazzo,[67] M. Perl,[67] S. Petrak,[67] B. N. Ratcliff,[67] A. Roodman,[67] A. A. Salnikov,[67]
R. H. Schindler,[67] J. Schwiening,[67] G. Simi,[67] A. Snyder,[67] A. Soha,[67] J. Stelzer,[67] D. Su,[67] M. K. Sullivan,[67] J. Va'vra,[67]
S. R. Wagner,[67] M. Weaver,[67] A. J. R. Weinstein,[67] W. J. Wisniewski,[67] M. Wittgen,[67] D. H. Wright,[67] A. K. Yarritu,[67]
C. C. Young,[67] P. R. Burchat,[68] A. J. Edwards,[68] T. I. Meyer,[68] B. A. Petersen,[68] C. Roat,[68] S. Ahmed,[69] M. S. Alam,[69]
J. A. Ernst,[69] M. A. Saeed,[69] M. Saleem,[69] F. R. Wappler,[69] W. Bugg,[70] M. Krishnamurthy,[70] S. M. Spanier,[70]
R. Eckmann,[71] H. Kim,[71] J. L. Ritchie,[71] A. Satpathy,[71] R. F. Schwitters,[71] J. M. Izen,[72] I. Kitayama,[72] X. C. Lou,[72]
S. Ye,[72] F. Bianchi,[73] M. Bona,[73] F. Gallo,[73] D. Gamba,[73] L. Bosisio,[74] C. Cartaro,[74] F. Cossutti,[74] G. Della Ricca,[74]
S. Dittongo,[74] S. Grancagnolo,[74] L. Lanceri,[74] P. Poropat,[74,§] L. Vitale,[74] G. Vuagnin,[74] R. S. Panvini,[75] Sw. Banerjee,[76]
C. M. Brown,[76] D. Fortin,[76] P. D. Jackson,[76] R. Kowalewski,[76] J. M. Roney,[76] R. J. Sobie,[76] H. R. Band,[77] B. Cheng,[77]
S. Dasu,[77] M. Datta,[77] A. M. Eichenbaum,[77] M. Graham,[77] J. J. Hollar,[77] J. R. Johnson,[77] P. E. Kutter,[77] H. Li,[77] R. Liu,[77]
A. Mihalyi,[77] A. K. Mohapatra,[77] Y. Pan,[77] R. Prepost,[77] P. Tan,[77] J. H. von Wimmersperg-Toeller,[77] J. Wu,[77] S. L. Wu,[77]
Z. Yu,[77] M. G. Greene,[78] and H. Neal[78]

(*B*A*B*AR Collaboration)

[1]*Laboratoire de Physique des Particules, F-74941 Annecy-le-Vieux, France*
[2]*Università di Bari, Dipartimento di Fisica and INFN, I-70126 Bari, Italy*
[3]*Institute of High Energy Physics, Beijing 100039, China*
[4]*University of Bergen, Inst. of Physics, N-5007 Bergen, Norway*
[5]*Lawrence Berkeley National Laboratory and University of California, Berkeley, California 94720, USA*
[6]*University of Birmingham, Birmingham, B15 2TT, United Kingdom*
[7]*Ruhr Universität Bochum, Institut für Experimentalphysik 1, D-44780 Bochum, Germany*
[8]*University of Bristol, Bristol BS8 1TL, United Kingdom*
[9]*University of British Columbia, Vancouver, BC, Canada V6T 1Z1*
[10]*Brunel University, Uxbridge, Middlesex UB8 3PH, United Kingdom*
[11]*Budker Institute of Nuclear Physics, Novosibirsk 630090, Russia*
[12]*University of California at Irvine, Irvine, California 92697, USA*
[13]*University of California at Los Angeles, Los Angeles, California 90024, USA*
[14]*University of California at Riverside, Riverside, California 92521, USA*
[15]*University of California at San Diego, La Jolla, California 92093, USA*
[16]*University of California at Santa Barbara, Santa Barbara, California 93106, USA*
[17]*University of California at Santa Cruz, Institute for Particle Physics, Santa Cruz, California 95064, USA*
[18]*California Institute of Technology, Pasadena, California 91125, USA*
[19]*University of Cincinnati, Cincinnati, Ohio 45221, USA*
[20]*University of Colorado, Boulder, Colorado 80309, USA*
[21]*Colorado State University, Fort Collins, Colorado 80523, USA*
[22]*Technische Universität Dresden, Institut für Kern- und Teilchenphysik, D-01062 Dresden, Germany*

[23]*Ecole Polytechnique, LLR, F-91128 Palaiseau, France*

[24]*University of Edinburgh, Edinburgh EH9 3JZ, United Kingdom*

[25]*Università di Ferrara, Dipartimento di Fisica and INFN, I-44100 Ferrara, Italy*

[26]*Florida A&M University, Tallahassee, Florida 32307, USA*

[27]*Laboratori Nazionali di Frascati dell'INFN, I-00044 Frascati, Italy*

[28]*Università di Genova, Dipartimento di Fisica and INFN, I-16146 Genova, Italy*

[29]*Harvard University, Cambridge, Massachusetts 02138, USA*

[30]*Universität Heidelberg, Physikalisches Institut, Philosophenweg 12, D-69120 Heidelberg, Germany*

[31]*Imperial College London, London, SW7 2AZ, United Kingdom*

[32]*University of Iowa, Iowa City, Iowa 52242, USA*

[33]*Iowa State University, Ames, Iowa 50011-3160, USA*

[34]*Università di Perugia, Dipartimento di Fisica and INFN, I-06100 Perugia, Italy*

[35]*Laboratoire de l'Accélérateur Linéaire, F-91898 Orsay, France*

[36]*Lawrence Livermore National Laboratory, Livermore, California 94550, USA*

[37]*University of Liverpool, Liverpool L69 72E, United Kingdom*

[38]*Queen Mary, University of London, E1 4NS, United Kingdom*

[39]*University of London, Royal Holloway and Bedford New College, Egham, Surrey TW20 0EX, United Kingdom*

[40]*University of Louisville, Louisville, Kentucky 40292, USA*

[41]*University of Manchester, Manchester M13 9PL, United Kingdom*

[42]*University of Maryland, College Park, Maryland 20742, USA*

[43]*University of Massachusetts, Amherst, Massachusetts 01003, USA*

[44]*Massachusetts Institute of Technology, Laboratory for Nuclear Science, Cambridge, Massachusetts 02139, USA*

[45]*McGill University, Montréal, QC, Canada H3A 2T8*

[46]*Università di Milano, Dipartimento di Fisica and INFN, I-20133 Milano, Italy*

[47]*University of Mississippi, University, Mississippi 38677, USA*

[48]*Université de Montréal, Laboratoire René J. A. Lévesque, Montréal, QC, Canada H3C 3J7*

[49]*Mount Holyoke College, South Hadley, Massachusetts 01075, USA*

[50]*Università di Napoli Federico II, Dipartimento di Scienze Fisiche and INFN, I-80126, Napoli, Italy*

[51]*NIKHEF, National Institute for Nuclear Physics and High Energy Physics, NL-1009 DB Amsterdam, The Netherlands*

[52]*University of Notre Dame, Notre Dame, Indiana 46556, USA*

[53]*The Ohio State University, Columbus, Ohio 43210, USA*

[54]*University of Oregon, Eugene, Oregon 97403, USA*

[55]*Università di Padova, Dipartimento di Fisica and INFN, I-35131 Padova, Italy*

[56]*Universités Paris VI et VII, Laboratoire de Physique Nucléaire et de Hautes Energies, F-75252 Paris, France*

[57]*Università di Pavia, Dipartimento di Elettronica and INFN, I-27100 Pavia, Italy*

[58]*University of Pennsylvania, Philadelphia, Pennsylvania 19104, USA*

[59]*Università di Pisa, Dipartimento di Fisica, Scuola Normale Superiore and INFN, I-56127 Pisa, Italy*

[60]*Prairie View A&M University, Prairie View, Texas 77446, USA*

[61]*Princeton University, Princeton, New Jersey 08544, USA*

[62]*Università di Roma La Sapienza, Dipartimento di Fisica and INFN, I-00185 Roma, Italy*

[63]*Universität Rostock, D-18051 Rostock, Germany*

[64]*Rutherford Appleton Laboratory, Chilton, Didcot, Oxon, OX11 0QX, United Kingdom*

[65]*DSM/Dapnia, CEA/Saclay, F-91191 Gif-sur-Yvette, France*

[66]*University of South Carolina, Columbia, South Carolina 29208, USA*

[67]*Stanford Linear Accelerator Center, Stanford, California 94309, USA*

[68]*Stanford University, Stanford, California 94305-4060, USA*

[69]*State University of New York, Albany, New York 12222, USA*

[70]*University of Tennessee, Knoxville, Tennessee 37996, USA*

[71]*University of Texas at Austin, Austin, Texas 78712, USA*

[72]*University of Texas at Dallas, Richardson, Texas 75083, USA*

[73]*Università di Torino, Dipartimento di Fisica Sperimentale and INFN, I-10125 Torino, Italy*

[74]*Università di Trieste, Dipartimento di Fisica and INFN, I-34127 Trieste, Italy*

[75]*Vanderbilt University, Nashville, Tennessee 37235, USA*

[76]*University of Victoria, Victoria, BC, Canada V8W 3P6*

[77]*University of Wisconsin, Madison, Wisconsin 53706, USA*

[78]*Yale University, New Haven, Connecticut 06511, USA*

With a sample of about 227×10^6 $B\bar{B}$ pairs recorded with the *BABAR* detector we perform a full angular analysis of the decay $B^0 \to \phi K^{*0}(892)$. We make novel measurements of five parameters sensitive to *CP* violation. We also measure the branching fraction to be $(9.2 \pm 0.9 \pm 0.5) \times 10^{-6}$ and

determine the fractions of longitudinal and parity-odd transverse contributions as $f_L = 0.52 \pm 0.05 \pm 0.02$ and $f_\perp = 0.22 \pm 0.05 \pm 0.02$. The phases of the parity-even and parity-odd transverse amplitudes relative to the longitudinal amplitude are found to be $\phi_\parallel = 2.34^{+0.23}_{-0.20} \pm 0.05$ rad and $\phi_\perp = 2.47 \pm 0.25 \pm 0.05$ rad. We also observe the decay $B^0 \to \phi K^{*0}(1430)$.

We make novel measurements of five parameters sensitive to *CP* violation in the angular analysis of the *B* decays [1], while improving knowledge of the decay rate, polarization, and final-state interactions. Angular correlation and asymmetry measurements in decays such as $B \to \phi K^*(892)$, which are expected to arise only from virtual loop effects in the standard model, are particularly sensitive to contributions from beyond the standard model [1]. The first evidence for this decay was provided by the CLEO [2] and *BABAR* [3] experiments. The large fraction of transverse polarization observed by *BABAR* [4] and confirmed by BELLE [5] enables a full angular analysis described by ten parameters for contributing amplitudes and their relative phases.

The angular distribution of the $B \to \phi K^*$ decay products can be expressed as a function of $\mathcal{H}_i = \cos\theta_i$ and Φ, where θ_i is the angle between the direction of the K from the $K^* \to K\pi$ (θ_1) or $\phi \to K\overline{K}$ (θ_2) and the direction opposite the B in the vector resonance rest frame, and Φ is the angle between the two resonance decay planes. The differential decay width has three complex amplitudes A_λ corresponding to the vector meson helicity $\lambda = 0$ or ± 1 [1,6]. When the last two are expressed in terms of $A_{\parallel,\perp} = (A_{+1} \pm A_{-1})/\sqrt{2}$ we have

$$\frac{8\pi}{9\Gamma} \frac{d^3\Gamma}{d\mathcal{H}_1 d\mathcal{H}_2 d\Phi} = \frac{1}{|A_0|^2 + |A_\parallel|^2 + |A_\perp|^2} \times \Big\{ |A_0|^2 \mathcal{H}_1^2 \mathcal{H}_2^2 + \frac{1}{4}(|A_\parallel|^2 + |A_\perp|^2)(1 - \mathcal{H}_1^2)(1 - \mathcal{H}_2^2) + \frac{1}{4}(|A_\parallel|^2$$
$$- |A_\perp|^2)(1 - \mathcal{H}_1^2)(1 - \mathcal{H}_2^2)\cos 2\Phi - \text{Im}(A_\perp A_\parallel^*)(1 - \mathcal{H}_1^2)(1 - \mathcal{H}_2^2)\sin 2\Phi$$
$$+ \sqrt{2}\text{Re}(A_\parallel A_0^*)\mathcal{H}_1 \mathcal{H}_2 \sqrt{1 - \mathcal{H}_1^2}\sqrt{1 - \mathcal{H}_2^2}\cos\Phi$$
$$- \sqrt{2}\text{Im}(A_\perp A_0^*)\mathcal{H}_1 \mathcal{H}_2 \sqrt{1 - \mathcal{H}_1^2}\sqrt{1 - \mathcal{H}_2^2}\sin\Phi \Big\}. \tag{1}$$

In this analysis, we measure the branching fraction, obtained from the number of signal events n_{sig}, the polarization parameters $f_L = |A_0|^2/\Sigma|A_\lambda|^2$, $f_\perp = |A_\perp|^2/\Sigma|A_\lambda|^2$, and the relative phases $\phi_\parallel = \arg(A_\parallel/A_0)$, $\phi_\perp = \arg(A_\perp/A_0)$. We allow for *CP*-violating differences between the $\overline{B}^0$ ($Q = +1$) and B^0 ($Q = -1$) decay amplitudes ($\overline{A}_\lambda$ and A_λ), where the flavor sign Q is determined in the self-tagging final-state with a $\overline{K}^*$ or K^*:

$$n_{\text{sig}}^Q = n_{\text{sig}}(1 + Q\mathcal{A}_{\text{CP}})/2; \tag{2}$$

$$f_L^Q = f_L(1 + Q\mathcal{A}_{CP}^0); \qquad f_\perp^Q = f_\perp(1 + Q\mathcal{A}_{CP}^\perp);$$
$$\phi_\parallel^Q = \phi_\parallel + Q\Delta\phi_\parallel; \qquad \phi_\perp^Q = \phi_\perp + \frac{\pi}{2} + Q\Big(\Delta\phi_\perp + \frac{\pi}{2}\Big).$$

If one loop diagram dominates the decay amplitude, the three direct *CP* asymmetries $\mathcal{A}_{CP}$, $\mathcal{A}_{CP}^0$, and $\mathcal{A}_{CP}^\perp$, and the two weak-phase differences $\Delta\phi_\parallel$ and $\Delta\phi_\perp$ are expected to be negligible. From the above parameters one can derive vector triple-product asymmetries $\mathcal{A}_T^\parallel$ and $\mathcal{A}_T^0$ as discussed in Ref. [1]:

$$\mathcal{A}_T^{\parallel,0} = \frac{1}{2}\Big(\frac{\text{Im}(A_\perp A_{\parallel,0}^*)}{\Sigma|A_\lambda|^2} + \frac{\text{Im}(\overline{A}_\perp \overline{A}_{\parallel,0}^*)}{\Sigma|\overline{A}_\lambda|^2} \Big). \tag{3}$$

We use data collected with the *BABAR* detector [7] at the PEP-II asymmetric-energy e^+e^- collider [8] operated at the center-of-mass (c.m.) energy of the $\Upsilon(4S)$ resonance ($\sqrt{s} = 10.58$ GeV). These data represent an integrated luminosity of about 205 fb^{-1}, corresponding to $(226.6 \pm 2.5) \times 10^6$ $B\overline{B}$ pairs. Charged-particle momenta are measured in a tracking system consisting of a five-layer double-sided silicon vertex tracker and a 40-layer drift chamber, both immersed in a 1.5-T solenoidal magnetic field. Charged-particle identification is provided by measurements of the energy loss in the tracking devices and by a ring-imaging Cherenkov detector.

We fully reconstruct $\overset{(-)}{B}{}^0 \to \phi \overset{(-)}{K}{}^{*0}$ candidates from their decay products $\phi \to K^+ K^-$ and $\overset{(-)}{K}{}^{*0} \to K^\pm \pi^\pm$. Charged track candidates are required to originate from a single vertex near the interaction point. We identify *B* meson candidates kinematically using the beam-energy-substituted mass $m_{\text{ES}} = [(s/2 + \mathbf{p}_i \cdot \mathbf{p}_B)^2/E_i^2 - \mathbf{p}_B^2]^{1/2}$ and the energy difference $\Delta E = (E_i E_B - \mathbf{p}_i \cdot \mathbf{p}_B - s/2)/\sqrt{s}$, where $(E_i, \mathbf{p}_i)$ is the initial state four-momentum obtained from the beam momenta, and $(E_B, \mathbf{p}_B)$ is the four-momentum of the reconstructed *B* candidate. The requirements on the ϕ and K^* invariant masses are $0.99 < m_{K\overline{K}} < 1.05$ and $0.75 < m_{K\pi} < 1.05$ (GeV). The selection window is $1.13 < m_{K\pi} < 1.73$ (GeV) in the study of the higher-mass K^* resonances.

To reject the dominant quark-antiquark continuum background, we require $|\cos\theta_T| < 0.8$, where θ_T is the angle between the B-candidate thrust axis and that of the rest of the tracks and neutral clusters in the event, calculated in the c.m. frame. We also construct a Fisher discriminant, $\mathcal{F}$, further discriminating between signal and background, that combines the following variables: the polar angles of the B-momentum vector and the B-candidate thrust axis with respect to the beam axis in the c.m. frame, and the two Legendre moments L_0 and L_2 of the energy flow around the B-candidate thrust axis [9].

Contamination from other B decays is small (about 2% of the total background) according to Monte Carlo (MC) simulation [10] and is taken into account in the fit described below. We remove signal candidates that have decay products with invariant mass within 12 MeV of the nominal mass values for $D_s^\pm$ or $D^\pm \to \phi\pi^\pm$.

We use an unbinned, extended maximum-likelihood fit to extract simultaneously the signal yield and angular distributions from a sample of selected events. There are several event categories j: signal, continuum $q\bar{q}$, combinatoric $B\bar{B}$ background, $B \to \phi K\pi$ with a nonresonant S-wave $K^\pm\pi^\mp$ contribution, and $B \to f_0(980)K^*$ with a broad S-wave K^+K^- contribution. The likelihood for each candidate i is defined as $\mathcal{L}_i = \sum_{j,k} n_j^k \mathcal{P}_j^k(\vec{x}_i; \vec{\alpha}; \vec{\beta})$, where each of the $\mathcal{P}_j^k(\vec{x}_i; \vec{\alpha}; \vec{\beta})$ is the probability density function (PDF) for variables $\vec{x}_i = \{m_{ES}, \Delta E, \mathcal{F}, m_{K\pi}, m_{K\bar{K}}, \mathcal{H}_1, \mathcal{H}_2, \Phi, Q\}$. The flavor index k corresponds to the measured value of Q, that is $\mathcal{P}_j^k \equiv \mathcal{P}_j \times \delta_{kQ}$. The n_j^k is the number of events with the flavor k in the category j.

The correlations among the fit input variables in the data are found to be small (less than 4%). The PDF $\mathcal{P}_j^k(\vec{x}_i; \vec{\alpha}; \vec{\beta})$ for a given candidate i is the product of the PDFs for each of the variables and a joint PDF for the helicity angles and resonance masses as discussed below. The signal angular distributions are parametrized with the set $\vec{\alpha} = \{f_L, f_\perp, \phi_\parallel, \phi_\perp, \mathcal{A}_{CP}^0, \mathcal{A}_{CP}^\perp, \Delta\phi_\parallel, \Delta\phi_\perp\}$ which are left free to vary in the fit. The other PDF parameters $\vec{\beta}$ describe the signal and background distributions discussed below. They are extracted from MC simulation or from data in m_{ES} and ΔE sidebands and are fixed in the fit. The MC resolutions are adjusted by comparing data and MC simulation in calibration channels with similar kinematics and topology, such as $B^0 \to D^-\pi^+$ with $D^- \to K^+\pi^-\pi^-$. The PDF parametrization for each event candidate accounts for the loss of acceptance near $\mathcal{H}_1 = 0.8$ due to the $D_s^\pm$ and $D^\pm$ rejection requirements.

We use a three-dimensional description for the helicity part of the signal PDF, using the ideal angular distribution from Eq. (1) multiplied by an acceptance function $\mathcal{G}(\mathcal{H}_1, \mathcal{H}_2, \Phi)$ parametrized with empirical polynomial functions. The detector acceptance effects are found to be

TABLE I. Summary of the $B^0 \to \phi K^{*0}(892)$ fit results. We show results for the ten primary signal fit parameters defined in Eq. (2) and the derived parameters: reconstruction efficiency ϵ which depends on decay polarization, branching fraction $\mathcal{B}$, and triple-product asymmetries from Eq. (3). All results include systematic errors, which are quoted last. The dominant correlation coefficients are given in the last column, they are also -34% for $\{\phi_\parallel, \Delta\phi_\parallel\}$, -51% for $\{\phi_\perp, \Delta\phi_\perp\}$, -42% for $\{\phi_\parallel, \Delta\phi_\perp\}$, and -40% for $\{\phi_\perp, \Delta\phi_\parallel\}$.

Fit parameter	Fit result	Correlation
$n_{\rm sig}$ (events)	$201 \pm 20 \pm 6$	
f_L	$0.52 \pm 0.05 \pm 0.02$	$\left.\vphantom{\begin{matrix}a\\b\end{matrix}}\right\}-46\%$
$f_\perp$	$0.22 \pm 0.05 \pm 0.02$	
$\phi_\parallel$ (rad)	$2.34^{+0.23}_{-0.20} \pm 0.05$	$\left.\vphantom{\begin{matrix}a\\b\end{matrix}}\right\}+70\%$
$\phi_\perp$ (rad)	$2.47 \pm 0.25 \pm 0.05$	
$\mathcal{A}_{CP}$	$-0.01 \pm 0.09 \pm 0.02$	
$\mathcal{A}_{CP}^0$	$-0.06 \pm 0.10 \pm 0.01$	$\left.\vphantom{\begin{matrix}a\\b\end{matrix}}\right\}-45\%$
$\mathcal{A}_{CP}^\perp$	$-0.10 \pm 0.24 \pm 0.05$	
$\Delta\phi_\parallel$ (rad)	$0.27^{+0.20}_{-0.23} \pm 0.05$	$\left.\vphantom{\begin{matrix}a\\b\end{matrix}}\right\}+70\%$
$\Delta\phi_\perp$ (rad)	$0.36 \pm 0.25 \pm 0.05$	
ϵ (%)	9.7 ± 0.5	
$\mathcal{B}$	$(9.2 \pm 0.9 \pm 0.5) \times 10^{-6}$	
$\mathcal{A}_T^\parallel$	$-0.02 \pm 0.04 \pm 0.01$	
$\mathcal{A}_T^0$	$+0.11 \pm 0.05 \pm 0.01$	

uniform in Φ, and we factor the $\mathcal{H}_1$ and $\mathcal{H}_2$ dependence as $\mathcal{G} \equiv \mathcal{G}_1(\mathcal{H}_1) \times \mathcal{G}_2(\mathcal{H}_2)$. We use two Gaussian functions for the parametrization of the signal PDFs for ΔE, m_{ES}, and $\mathcal{F}$. A relativistic P-wave Breit-Wigner distribution, convoluted with a Gaussian resolution function, is used for the resonance masses.

Parametrization of the nonresonant B-decay contributions is identical to that of the signal for m_{ES}, ΔE, and $\mathcal{F}$, but is different for the angular and invariant mass distributions. In particular, a broad invariant mass distribution accounts for all potential S-wave contributions leaking into the mass selection window. For the combinatorial background, we use polynomials, except for m_{ES} and $\mathcal{F}$ distributions which are parametrized by an empirical phase-space function and by the two Gaussian functions, respectively. Resonance production occurs in the background and this is taken into account in the PDF. The background $\mathcal{H}_i$ distribution is separated into contributions from combinatorial background and from real vector mesons.

We allow for multiple candidates in a given event by assigning to each a weight of $1/N_i$, where N_i is the number of candidates in the same event. The average number of candidates per event is 1.04. The extended likelihood for a sample of $N_{\rm cand}$ candidates is

$$\mathcal{L} = \exp\left(-\sum_j n_j\right) \prod_{i=1}^{N_{\rm cand}} \exp\left(\frac{\ln\mathcal{L}_i}{N_i}\right). \tag{4}$$
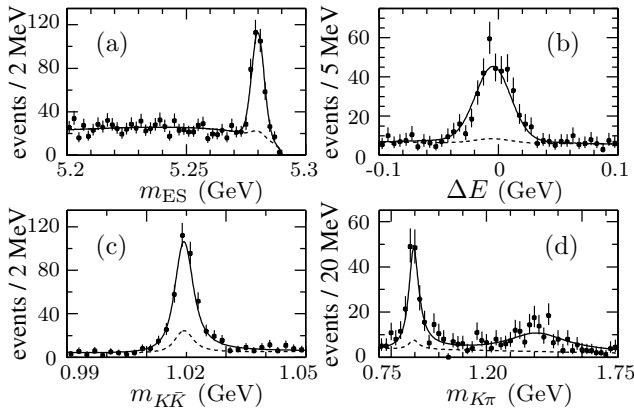
FIG. 1.　Projections onto the variables m_{ES} (a), ΔE (b), $m_{K\bar{K}}$ (c), and $m_{K\pi}$ (d) for the signal $B^0 \to \phi K^{*0}(892)$ and $\phi K^{*0}(1430)$ candidates combined.
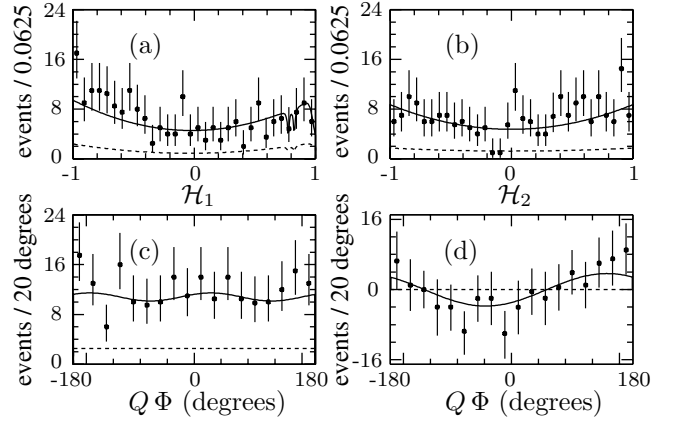

FIG. 2.　Projections onto the variables $\mathcal{H}_1$ (a), $\mathcal{H}_2$ (b), $Q\Phi$ (c), and the differences between the $Q\Phi$ projections for events with $\mathcal{H}_1\mathcal{H}_2 > 0$ and with $\mathcal{H}_1\mathcal{H}_2 < 0$ (d) for the signal $B^0 \to \phi K^{*0}(892)$ candidates.

The event yields n_j, asymmetries $\mathcal{A}_j$, and the signal polarization parameters $\vec{\alpha}$ are obtained by maximizing the likelihood $\mathcal{L}$.

The results of our maximum-likelihood fit to the sample of $B^0 \to \phi K^{*0}(892)$ candidates are summarized in Table I. We also repeat the fit with the requirement $1.13 < m_{K\pi} < 1.73$ (GeV) and without the angular information. We observe 181 ± 17 events (statistical errors only) of the decays $B^0 \to \phi K^{*0}(1430)$ with statistical significance greater than 10σ. In Figs. 1–3 we show projections onto the variables, where data distributions are shown with a requirement on the signal-to-background probability ratio $\mathcal{P}_{sig}/\mathcal{P}_{bkg}$ calculated with the plotted variable excluded. The solid (dashed) lines show the signal-plus-background (background) PDF projections.

In the analysis of the decay $B^0 \to \phi K^{*0}(892)$ for any given set of values $(\phi_\parallel, \phi_\perp, \Delta\phi_\parallel, \Delta\phi_\perp)$ simple transformations of the angles, for example, $(-\phi_\parallel, \pi - \phi_\perp, -\Delta\phi_\parallel, -\Delta\phi_\perp)$, give rise to other sets of values which satisfy Eq. (1) in an identical manner. To resolve this ambiguity, the set of values lying closest to the theoretical expectation $(\pi, \pi, 0, 0)$ [1,6,11] is chosen. In Fig. 4 we show likelihood function contour plots.

We find the decay $B^0 \to \phi K^{*0}(1430)$ to be predominantly longitudinally polarized based on the $\mathcal{H}_2$ angular distribution in Fig. 3(b). The width [12] and the angular distribution of the $K^{*0}(1430)$ resonance structure are not consistent with the pure $K_2^{*0}(1430)$ tensor state at more than 10σ. However, the angular distribution provides evidence (with statistical significance of 3.2σ) of the longitudinally polarized tensor $K_2^{*0}(1430)$ contribution in addition to the scalar $K_0^{*0}(1430)$; see Fig. 3(a).

Our $B^0 \to \phi K^{*0}(892)$ fit is performed with the $B \to f_0 K^*$ and $B \to \phi K\pi$ contributions unconstrained. We obtain the event yields 25 ± 10 and 11 ± 15, respectively. The systematic uncertainties due to interference are estimated using generated samples with conservative assumptions about the S-wave intensity and the interference phase. Additional systematic uncertainty originating from B background is taken as the difference between the fit results with the combinatoric $B\overline{B}$ background component fixed to zero and the expectation from MC.

We vary the PDF parameters within their respective uncertainties, and derive the associated systematic errors. The biases from the finite resolution of the helicity angle measurement, the dilution due to the presence of fake combinations, or other imperfections in the signal PDF model are estimated with MC simulation and are found to be relatively small.

The systematic errors in efficiencies are dominated by those in track finding and particle identification. Other systematic effects arise from event-selection criteria, ϕ and K^{*0} branching fractions, MC statistics, and number of B mesons. We calculate the efficiencies using the measured polarization and assign a systematic error corresponding to the total polarization uncertainty. We find the uncertainty in the charge asymmetry due to the track reconstruction and identification to be less than 0.02.
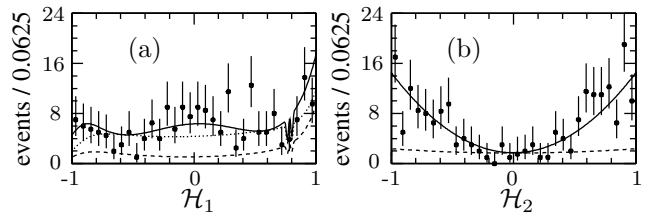

FIG. 3.　Projections onto the variables $\mathcal{H}_1$ (a) and $\mathcal{H}_2$ (b) for the signal $B^0 \to \phi K^{*0}(1430)$ candidates. The difference between the solid and dotted lines in (a) shows the contribution of the tensor state to the angular distribution.
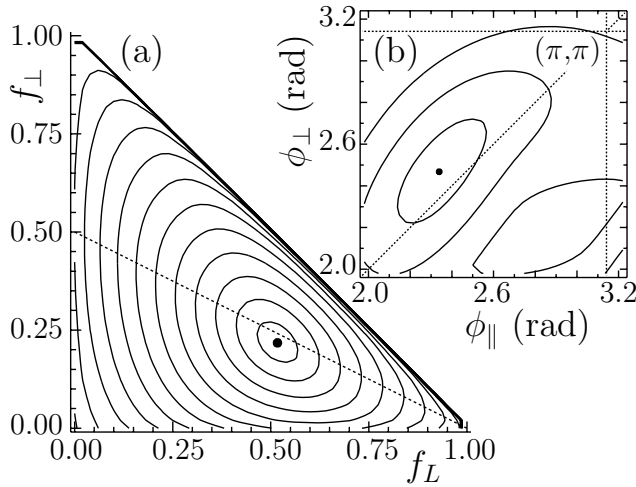
FIG. 4. Likelihood function contours with 1σ intervals for polarization (a) and phase (b) measurements in the $B^0 \to \phi K^{*0}(892)$ analysis. The fit results are shown with dots. Diagonal dashed lines $f_\perp = (1 - f_L)/2$ and $\phi_\perp = \phi_\parallel$ correspond to $|A_{+1}| \gg |A_{-1}|$. In (b) the (π, π) point is indicated by the crossed dashed lines.

In summary, we have performed a full angular analysis and searched for CP violation in the angular distribution with the decays $\overset{(-)}{B^0} \to \overset{(-)}{\phi} K^{*0}(892)$. Our results are summarized in Table I. We observe, with more than 5σ significance, nonzero contributions from all of the three amplitudes $|A_0|$, $|A_\perp|$, and $|A_\parallel|$; see Fig. 4(a). We also find 3σ evidence for nonzero final-state-interaction phases, see Fig. 4(b). These results supersede our earlier measurements in this channel [3,4]. We also observe the decay $B^0 \to \phi K^{*0}(1430)$.

For B decays to light charmless particles we expect the hierarchy of decay amplitudes to be $|A_0| \gg |A_{+1}| \gg |A_{-1}|$ under the assumption of pure loop diagram contribution, which is analogous to the discussion in Refs. [6,11,13]. Our measurements with the decay $B^0 \to \phi K^{*0}(892)$ do not agree with the first inequality but agree with the previous measurements in Refs. [4,5]. This suggests other contributions to the decay amplitude, previously neglected, either within or beyond the standard model [1,13].

We would like to thank Yuval Grossman, Alexander Kagan, David London, Mahiko Suzuki, and Arkady Vainshtein for useful discussions. We are grateful for the excellent luminosity and machine conditions pro-

*Now at Department of Physics, University of Warwick, Coventry, United Kingdom.
†Also with Università della Basilicata, Potenza, Italy.
‡Also with IFIC, Instituto de Física Corpuscular, CSIC-Universidad de Valencia, Valencia, Spain.
§Deceased.
[1] G. Valencia, Phys. Rev. D **39**, 3339 (1989); A. Datta and D. London, Int. J. Mod. Phys. A **19**, 2505 (2004).
[2] CLEO Collaboration, R. A. Briere *et al.*, Phys. Rev. Lett. **86**, 3718 (2001).
[3] *BABAR* Collaboration, B. Aubert *et al.*, Phys. Rev. Lett. **87**, 151801 (2001); Phys. Rev. D **65**, 051101 (2002).
[4] *BABAR* Collaboration, B. Aubert *et al.*, Phys. Rev. Lett. **91**, 171802 (2003); hep-ex/0303020.
[5] BELLE Collaboration, K.-F. Chen *et al.*, Phys. Rev. Lett. **91**, 201801 (2003).
[6] G. Kramer and W. F. Palmer, Phys. Rev. D **45**, 193 (1992); H.-Y. Cheng and K.-C. Yang, Phys. Lett. B **511**, 40 (2001); C.-H. Chen, Y.-Y. Keum, and H-n. Li, Phys. Rev. D **66**, 054013 (2002).
[7] *BABAR* Collaboration, B. Aubert *et al.*, Nucl. Instrum. Methods Phys. Res., Sect. A **479**, 1 (2002).
[8] PEP-II Conceptual Design Report, SLAC-R-418, 1993.
[9] *BABAR* Collaboration, B. Aubert *et al.*, Phys. Rev. D **70**, 032006 (2004).
[10] The *BABAR* detector Monte Carlo simulation is based on GEANT4: GEANT4 Collaboration, S. Agostinelli *et al.*, Nucl. Instrum. Methods Phys. Res., Sect. A **506**, 250 (2003).
[11] A. Ali *et al.*, Z. Phys. C **1**, 269 (1979); M. Suzuki, Phys. Rev. D **66**, 054018 (2002).
[12] S. Eidelman *et al.*, Phys. Lett. B **592**, 1 (2004).
[13] A. Kagan, Phys. Lett. B **601**, 151 (2004); Y. Grossman, Int. J. Mod. Phys. A **19**, 907 (2004); P. Colangelo, F. De Fazio, and T. N. Pham, Phys. Lett. B **597**, 291 (2004).